Talanta 117 (2013) 139–145

Contents lists available at ScienceDirect

Talanta

journal homepage: www.elsevier.com/locate/talanta

An organic thin film photodiode as a portable photodetector for the detection of alkylphenol polyethoxylates by a flow fluorescence-immunoassay on magnetic microbeads in a microchannel

Ryoichi Ishimatsu [a], Azusa Naruse [a], Rong Liu [a], Koji Nakano [a], Masayuki Yahiro [b,c], Chihaya Adachi [a,c,d], Toshihiko Imato [a,*]

[a] Department of Applied Chemistry, Graduate School of Engineering, Kyushu University, 744 Motooka, Fukuoka 819-0395, Japan
[b] Institute of System, Information Technology and Nanotechnology, 744 Motooka, Fukuoka 819-0395, Japan
[c] Center for Organic Photonics and Electronics Research (OPERA), Kyushu University, 744 Motooka, Nishi, Fukuoka, Japan
[d] International Institute for Carbon-Neutral Energy Research (WPI-I^{2}CNER), Kyushu University, 744 Motooka, Nishi, Fukuoka, Japan

ARTICLE INFO

Article history:
Received 3 April 2013
Received in revised form
26 August 2013
Accepted 27 August 2013
Available online 3 September 2013

Keywords:
Organic photodiodes
Microchip
ELISA
Microbeads

ABSTRACT

An organic thin film photodiode (OPD) was successfully employed as a portable photodetector in a competitive enzyme-linked immunosorbent assay (ELISA) of a class of nonionic surfactants, namely alkylphenol polyethoxylates (APnEOs) which are an environmental pollutant. Microbeads that were chemically immobilized with an anti-APnEOs antibody were used in the assay. The OPD consisted of a layer of copper phthalocyanine (CuPc), C_{60} and a second layer of bathocuproine (BCP) with a bulk heterojunction composed of CuPc and C_{60} prepared by a vapor deposition method on an indium-tin oxide coated glass substrate. The OPD showed an incident photon-current efficiency (IPCE) of approximately 19% for light at a wavelength of 585 nm. This relatively high IPCE at 585 nm makes it suitable for detecting the fluorescence of resorufin (λ_{em}=585 nm), the product of the competitive ELISA, produced through the enzymatic reaction of Amplex Red with horseradish peroxidase (HRP) and H_2O_2. A fluorometric detector was assembled on a microchip by combining the fabricated OPD and a commercial LED as a photodetector and a light source, respectively. The photocurrent of the OPD due to the fluorescence of resorufin was proportional to the concentration of resorufin in the concentration range from 0 to 8 μM. When the fabricated OPD was used as a portable photodetector, the competitive ELISA of APnEOs using HRP labeled APnEOs (HRP–APnEOs) was performed on magnetic microbeads on which surface an anti-APnEOs antibody had been immobilized. A typical sigmoidal calibration curve was obtained and the data were in good agreement with a numerical simulation, where the photocurrent of the OPD was plotted against the concentration of APnEOs, determined via the competitive ELISA. The detection limit of the immunoassay for APnEOs was approximately 2 and 4 ppb in batch and flow system, respectively.

1. Introduction

Micro-total analysis systems [1] (μ-TAS) or a "lab-on-a-chip" can be used for the on-site analysis of environmental pollutants and bed-side diagnosis in the field of health care. In terms of portability, the detection system needs to be miniaturized, however, the current generation of optical instruments which being used for spectrometric detection is somewhat large and not really acceptable for on-site analyses. For the purpose of miniaturization, inorganic photodiodes have been employed for optical measurements such as detection based on fluorescence. For instance, Kamei et al. reported that a concentration of 7 nM fluorecein could be detected in a microchannel using a hydrogenated amorphous Si photodiode, whose absorbance in the visible region was higher than that of a single crystalline Si photodiode [2,3]. Fan et al. detected 0.09 fmol of fluorecein in an injection sample size of 0.37 nL in microchip electrophoresis by a light-emitting diode induced fluorescence detector in conjunction with a photodiode [4]. An avalanche photodiode was used to amplify the response of the photosignal, and 0.2 nM of fluorecein was detected [5].

Organic thin film photodiodes (OPDs) [6–10] have considerable promise for use as portable photodetectors as well as the inorganic photodiodes for spectrometry in measurements related to fluorescence, chemiluminescence, and UV–vis absorption. One of the unique features of OPDs is that one can easily tune the detection wavelength with tunable incident photon-current efficiency (IPCE)

* Corresponding author. Tel.: +81 92 802 2889; fax: +81 92 802 2889.
E-mail address: imato@cstf.kyushu-u.ac.jp (T. Imato).

0039-9140/$ - see front matter © 2013 Elsevier B.V. All rights reserved.
http://dx.doi.org/10.1016/j.talanta.2013.08.044

spectra by selecting type of organic thin layers for fabricating an appropriate OPD. This is a distinct advantage compared to inorganic photodiodes since the IPCE is related to the absorption spectrum of OPD organic thin films [8]. This feature enables to reduce the background photocurrent from the light source and to enhance in the photocurrent due to the fluorescence from the target compound by designing OPD having lower IPCE at excitation wavelength and higher IPCE at fluorescent wavelength, which may lead to a lower limit of detection. In addition to the tunability of OPDs, because of their compactness and ease of fabrication, OPDs are suitable for use as a portable photodetector in μ-TAS.

Because of its sensitivity and selectivity, the enzyme-linked immunosorbent assay (ELISA) [11] has been widely used for the determination of a variety of environmental pollutants and biologically important compounds. In the typical ELISA method, the products (the target antigens) produced as the result of an enzymatic reaction are detected based on spectrometric detection, such as absorbance, fluorescent and the chemiluminescent intensities of the products. A smaller, more portable and less expensive instrument equipped with OPDs as a photodetector would have the advantage of permitting an analysis to be performed on a microchip such as a μ-TAS. Therefore, performing ELISA on a microchip equipped with an OPD as a photodetector would result in a portable, selective and sensitive analytical tool suitable for on-site monitoring and bed side diagnosis. As of this writing, several examples of the use of OPDs as a photodetector for spectrometric analysis have appeared and demonstrated the validity of OPDs [12–15]. However, as far as we know, attempts to combine ELISA with the OPD are limited [16] including our previous research [17]. Ligler et al. reported on a chemiluminescence immunoassay for the detection of staphylococcal enterotoxin B at a concentration as low as 0.5 ng mL^{-1} by using a polymer-type OPD as the photodetector [16]. They successfully achieved such a low detection limit by suppressing both the background noise and dark current of the OPD by applying a small bias voltage (0–100 mV). We recently, reported on the fluorometric detection of IgA by sandwich-type ELISA on a polydimethylsiloxane (PDMS) microfluidic chip, where an OPD prepared by the vapor deposition of copper phthalocyanine (CuPc) and C_{60} was used [17]. In our case, a primary antibody (anti-IgA antibody) was immobilized on the surface of the PDMS chip through hydrophobic interactions, and a detection limit of 15 ng mL^{-1} of IgA was successfully achieved. The resulting detection limit is comparable to that for the case of an inorganic photodiode [18–22]. Far et al. quantitatively determined amphetamine in plasma and urine sample with a chemiluminescent immunoassay and obtained a detection limit of 6 ppb by using an inorganic photodiode [18].

Here we report on the fluorometric determination of alkylphenol polyethoxylates (APnEOs) based on competitive immunoreactions of HRP labeled APnEOs (HRP–APnEOs) and APnEOs on magnetic microbeads containing an immobilized anti-APnEOs antibody. The assay involved the enzymatic reaction of the labeled HRP with a substrate of Amplex Red in a PDMS microfluidic chip equipped with an OPD. APnEOs, which are a type of nonionic surfactant, are industrially used in a large quantities as detergents and dispersants [23a], and 80% of APnEOs for industrial use is nonylpnenolethoxylate in Japan [23b]. Toxicity of APnEOs is not so high compared with a class of alkylphenol such as nonlyphenol which is biodegradation products of APnEOs (lethal concentration 50, LC50, of nonylphenol is in the range of 130–1400 ppb for fish whereas 1–10 ppm of LC50 of nonlyppnenolethoxylate for fish) [23c]. In Japan, because of the toxicity, and the fact that nonylphenol is generated through biodegradation, nonylphenolethoxylate is registered in the list of in Priority Assessment Chemical Substances (PACSs) under the Chemical Substances Control Low [23d]. Thus, it is practically very important to determine APnEOs concentration to assess environmental pollution. In this study, instead of the physical adsorption of the antibody on the PDMS chip as was used in our previous research, the anti-APnEOs antibody was chemically attached to the surface of magnetic microbeads [24]. Magnetic microbeads have an advantage, in that they can be trapped and washed easily via the use of a magnet located under the microchip. Because of the larger surface area of the microbeads, the time required for the enzymatic reaction can be shortened considerably, and the reaction area can be controlled well (just on the magnetic microbeads). It is also possible to omit several cleaning steps that were required in our previously reported ELISA method, since the magnetic microbeads used in our assay are replaced with new magnetic microbeads. Therefore, using magnetic microbeads is advantageous for practical applications.

2. Experimental

2.1. Chemicals and materials

Hydrogen peroxide (30% aqueous solution), APnEOs, albumin from bovine serum (BSA, Cohn Fraction V, pH = 7.0), *N*-hydroxysuccinimide (NHS), and 1-ethyl-3-(3-dimethylaminopropyl) carbodiimide hydrochloride (EDC), tris(hydroxymethyl)aminomethane (Tris), HCl were purchased from Wako Pure Chemical Industries Ltd. Tween 20 and glycine (Gly) were obtained from Kishida Chemical Co. Ltd. HRP-APnEOs, anti-APnEOs antibody were received from Tokiwa Chemicals Industries Co. CuPc and bathocuproine (BCP) were obtained from Tokyo Chemical Industry Co., Ltd. C_{60} (99.95%) was purchased from Material Technologies Research Ltd. PDMS microchip was fabricated using Sylgard 184 Silicone Elastomer Kit (Dow Corning Corporation) containing a base agent (a mixture of silica and tetra(trimethyl) siloxysilane) and a curing agent (a mixture of silica and octamethylcyclotetrasiloxane). A peek tube (0.125 mm i.d., 0.159 mm o.d.) was obtained from IDEX Co. Al flaks (99.999%) were purchased from Nilaco Co. An aqueous suspension of magnetic microbeads coated with polylactic acid (d = 100 μm) was purchased from the Micromod Co. Bisphenol epoxy resin was received from Nagase Chemtex Co. Amplex Red was purchased from Fluka and resorufin was obtained from Sigma-Aldrich. The water used in this study was purified by means of a Milli-Q system (Millipore Co.). An indium-tin oxide (ITO, 100 nm thickness) coated glass plate was obtained from Sanyo Vacuum Industries Co., Ltd. and was cut at a size of 25 mm × 25 mm. All chemicals were used as received.

2.2. Fabrication of the OPD

We fabricated an OPD with a bulk heterojunction of CuPc and C_{60} by a vapor deposition method [25–28]. In the fabrication process of the OPD, CuPc, C_{60}, BCP and Al were successively deposited on a cut ITO glass using a vacuum evaporation system (E-110, ALS Technology) at a deposition rate of 0.02–0.04 nm s^{-1} under 10^{-3} Pa. The structure of the OPD fabricated in this work is as follows;

Glass|ITO (100 nm)|CuPc (15 nm)|CuPc:C_{60} = 3:2 (10 nm)|C_{60} (25 nm)|BCP (10 nm)|Al (80 nm).

The numbers in the parenthesis indicate the thickness of each deposited layer component. To form the bulk heterojunction of CuPc and C_{60}, two components were evaporated and simultaneously deposited by controlling the deposition rate. After the deposition of the Al layer, a glass plate was placed on the Al layer to seal the fabricated device by using a UV-cured resin in a glove box (KK-011 AS-Extra, ALS Technology). The fabricated OPD was stored in the dark until use.

2.3. Photocurrent–voltage characterization of OPD

The photocurrent–photovoltage characteristics of the fabricated OPD were determined by an AM 1.5 solar illumination (Otento-Sun II, KP type, Bunkokeik) with a Xe-lamp (Model XCS-150A, Jasco, Japan) and a source meter (R6423, Advantest). The photocurrents at different wavelengths were converted to IPCE, which was measured using the source meter under irradiation from a monochromatic light source (SK-U1152X, Ushio Inc.) and a monochrometor (SM-10P, Bunkokeiki) from 400 nm to 800 nm at intervals of 10 nm. A Si photodiode (BS-520, Bunkokeiki) was used to calibrate the incident light-power of the monochromatic light for calculating the conversion efficiency of the OPD.

2.4. Fabrication of microchannel chip

A PDMS chip with a Y-shaped channel was prepared by a conventional method using a template, as follows. The template was fabricated using a Y-shape acrylic plate which was fixed on a glass plate ($7.7 \times 5.2 \times 0.1$ cm^3) by an epoxy resin adhesive. The viscous mixture of the base and the curing agents in the PDMS kit at a weight ratio of 10:1 was poured onto the template which was then heated at 65 °C for 1.5 h to produce a PDMS chip with a thickness of ca. 5 mm. The PDMS chip was peeled off from the template and three holes for two inlets and one outlet ($d=1.5$ mm) were formed using a drill. The surface of the PDMS chip on the microchannel side was treated with an oxygen plasma. A glass plate ($7.7 \times 5.2 \times 0.1$ cm^3) coated with thin PDMS was subjected to plasma irradiation, and was placed on the PDMS chip and pressed by hand. The resulting PDMS chip was then placed in a drying oven at 120 °C for 6 h. The peek tubes were fixed in the holes of the PDMS by using a urethane resin adhesive (SU Clear, Konishi Co., Ltd.). The overall design of the microchannel is illustrated in Fig. 1(a).

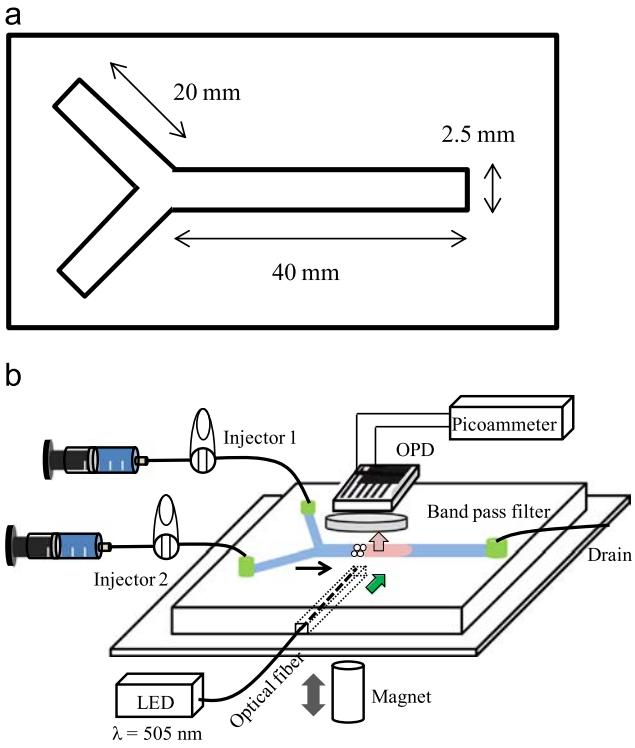

Fig. 1. Illustrations of the microchannel (a) and flow system for the detection of APnEOs (b). The depth of the microchannel is 650 μm.

2.5. Immobilization of anti-APnEOs antibody on microbeads

Magnetic microbeads ($d=100$ μm) with carboxyl groups on the surface were used for chemically immobilizing the anti-APnEOs antibody [29,30]. A schematic representation of the immobilization of the anti-APnEOs antibody on the surface of magnetic microbeads is shown in Scheme 1. A suspension of the microbeads (10 mg mL^{-1}, 200 μL) was washed three times with an imidazol-HCl buffer (pH=7.0, 1.0 mL) in a test tube before the amino coupling method as follows. Both 0.2 M NHS and 0.8 M EDC buffer solutions (imidazole-HCl at pH=7.0, 200 μL) were added to the test tube containing a suspension of microbeads, and the suspension incubated for 10 min at 37 °C to modify the surface of carboxyl group by succinimide. After the incubation, the microbeads were rinsed three times with the imidazol-HCl buffer. A solution of anti-APnEOs antibody in a buffer (400 μL, 1.0 ppm of imidazol-HCl at pH=7.0) was then added to the test tube, and the resulting suspension was kept at 25 °C for 24 h to chemically immobilize the anti-APnEOs antibody to the surface. After this immobilization procedure, the microbeads were rinsed three times with a Tris–HCl buffer solution (pH=8.0, 1.0 mL). The final stock suspension of the microbeads immobilized with the anti-APnEOs antibody was stored at 4 °C in a refrigerator until use.

2.6. Competitive ELISA for APnEOs

Amplex Red, which produces fluorescent resorufin by an enzymatic reaction with HRP in the presence of H_2O_2 (Scheme 2) [31a], was employed as a substrate of the competitive ELISA for the determination of APnEOs.

2.6.1. Batch system

A fluorometric batch system was constructed from a commercial LED light source with a center wavelength of 505 (LLS-505, KLV Co.) and 591 nm (yellow, the emission spectra is shown in Fig. S5) and the fabricated OPD as a fluorescence detector. The light from the LED was transmitted through an optical filter to a spectrofluorometric cell and the OPD was placed perpendicular against the LED light. In order to suppress the effects of incident light, a band pass filter (620 ± 30 nm, ET620/60 m, Chroma Technology Co.) was placed just in front of the OPD. An aliquot of a 1.0 mL of HRP–APnEOs (500 ppb) conjugate solution containing different concentrations of APnEOs (0–100 ppb) was added in a suspension of the magnetic microbeads immobilized with the anti-APnEOs antibody (2 mg mL^{-1}, 200 μL) and kept for 30 min at 25 °C to carry out the competitive immunoreaction between the anti-APnEOs antibody on the magnetic microbeads and the HRP–APnEOs conjugate and APnEOs. During the enzymatic reaction, the magnetic microbeads were on the bottom of

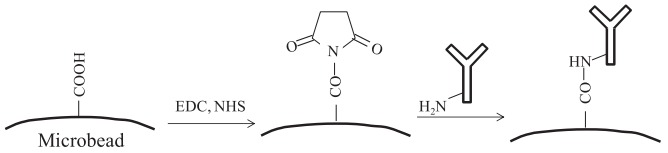

Scheme 1. Immobilization of an antibody on the surface of magnetic microbeads .

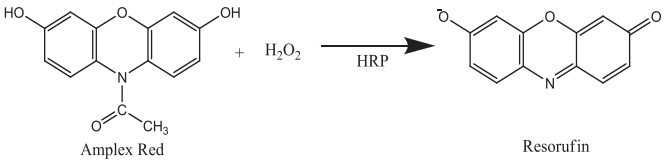

Scheme 2. Enzymatic reaction of Amplex Red with HRP and H_2O_2 .

cell. The microbeads were then rinsed six times with a Tris–HCl buffer solution (pH=8.0, 1.0 mL). After this washing, 1940 μL of Tris–HCl (pH=8.0) was added, and the suspension of the magnetic microbeads was transferred into a disposable spectrofluorometric cell ($1\times1\times5$ cm^3). Then, 60 μL of a mixed solution of Amplex Red (1.7 mM) and H_2O_2 (17 mM) was gently added to the cell. After standing for 500 s, the cell was irradiated with the LED light, and the photocurrent of the OPD due to resorufin generated from the enzymatic reaction of HRP on the magnetic microbeads with Amplex Red and H_2O_2 was recorded. The photocurrent was measured with a picoammeter (6485, TFF Co. Keithley Instruments).

2.6.2. Flow system

The flow injection system was constructed from two syringe pumps (SP-300, New Era System, Inc.) and two injectors (Rheodyne 9725, IDEX health and Science LCC) as schematically illustrated in Fig. 1(b). The carrier solution (Tris–HCl buffer at pH=8.0) was controlled by means of syringe pumps at rate of 20 μL min^{-1} from the inlet during the injections. A 100 μL aliquot of Gly–HCl buffer solution containing a 0.1% Tween 20 (pH=2.0) was first injected from injector 1 to avoid the physical adsorption of the HRP–APnEOs conjugate on the PDMS chip. Second, the suspension of magnetic microbeads, with the anti-APnEOs antibody immobilized on them (2 mg mL^{-1}, 100 μL) was injected from injector 1. The microbeads were trapped in the microchannel by a neodymium magnet (Magfine Co.) which was placed under the bottom of the PDMS microchip and whose up and down shift action were controlled by a solenoid. It took about 5 min for injected magnetic microbeads to reach the detection point. Third, 100 μL of a mixed solution of APnEOs and the HRP–APnEOs conjugate was injected from injector 1. The solution consisted of 0–100 ppb APnEOs and 500 ppb HRP–APnEOs prepared with Tris–HCl buffer (pH=8.0) and carrier solution flowed for 5 min to rinse the channel. Lastly, 100 μL of a mixed solution of 0.1 mM Amplex Red and 1 mM H_2O_2 (100 μL) was injected from injector 2. After the injection of this mixed solution, the magnetic microbeads were discarded with the carrier solution by shifting the magnet down. The side of the channel of the PDMS chip was irradiated with an LED light source. Namely, an optical fiber (100 μm core diameter), in which the end clad was peeled off, was inserted in a groove to approach near the sidewall of the microchannel. The tip of the optical fiber was located at a distance of 1 mm from the wall of the microchannel. The photocurrent of the OPD resulting from the fluorescence of resorufin, which was passed through the band pass filter, was recorded with the picoammeter.

3. Results and discussion

3.1. Characteristics of OPD

Fig. 2 shows the relationship between an IPCE and wavelength (IPCE spectrum) for the fabricated OPD. Two maxima were observed at around 450 and 620 nm. It is known that the IPCE spectrum depends on the absorption property of the components of the OPDs, and in this case, these maxima, at around 450 and 620 nm, can be assigned to the absorption maxima of spectra of C_{60} and CuPc, respectively [8,28]. The open-circuit voltage (V_{oc}) and the short-circuit current density (I_{sc}) of the OPD were 0.41 V and 5.2 mA cm^{-2} respectively. The conversion efficiency estimated from the $I_{sc}-V_{oc}$ characteristic curve was 0.86% and the fill factor was 0.40.

The absorbance and fluorescence spectra of resorufin, which is a product of the enzymatic reaction of Amplex Red, are also shown in Fig. 2. The maxima for the absorbance and fluorescence were at 570 and 585 nm, respectively, and the IPCE of the fabricated OPD

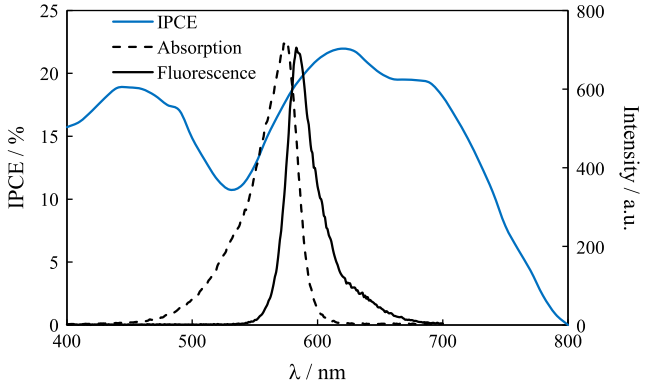

Fig. 2. The IPCE spectrum of OPD with a bulk heterojunction of C_{60} and BCP, and excitation and the emission spectra of 10 μM resorufin.

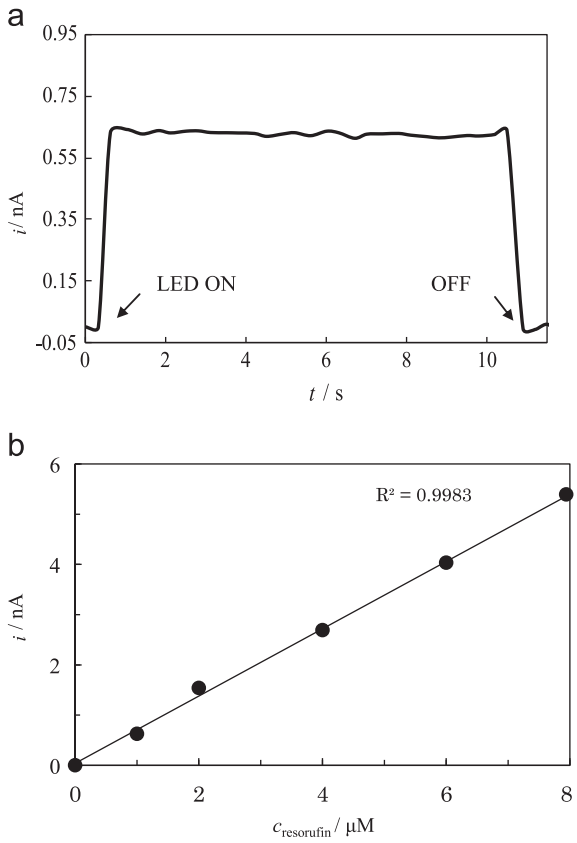

Fig. 3. (a) Photocurrent response for the fluorescence of resorufin and (b) photocurrent response as a function of concentration of resorufin with an LED (λ=591 nm) irradiation.

at 585 nm was about 19%. This indicates that the fluorescence due to resorufin can be efficiently converted into a photocurrent. Two commercial LEDs (λ=505 and 591 nm) were used as a light source for the measurement and the values of IPCE at these wavelength were 13% and 20% respectively.

3.2. Competitive ELISA for APnEOs in a batch system

First, to evaluate the performance of the OPD, the photocurrent due to the fluorescence of resorufin at different concentrations was determined using the yellow LED (591 nm) as the excitation light. The photocurrent response of the OPD due to the fluorescence of resorufin is shown in Fig. 3. As can be seen from Fig. 3(a), the OPD responds to the fluorescence light very rapidly and its signal was stable. The average values of the photocurrent for 10 s

at the plateau region were plotted against the concentrations of resorufin, as shown in Fig. 3(b). A good linearity was observed between the photocurrent and the concentration of resorufin, indicating that the fabricated OPD is a good candidate for use in fluorometric detection.

The OPD was employed as the photodetector for the competitive ELISA for APnEOs in a batch system. The amount of anti-APnEOs antibody immobilized on the magnetic microbeads was estimated through the antigen–antibody reaction with the HRP–APnEOs conjugate. Namely, the time-dependent photocurrent of the fabricated OPD due to fluorescent resorufin was first measured by the addition of the HRP–APnEOs solutions to the mixed solution of Amplex Red and H_2O_2, and the reaction rates for the time-dependent photocurrent produced were calculated. Second, after incubating the magnetic microbeads immobilized with the anti-APnEOs antibody with an excess of the HRP–APnEOs and washing with the buffer solution, a mixed solution of Amplex Red and H_2O_2 was added to a suspension of the magnetic microbeads in the spectrofluorometric cell. The time-dependent photocurrent of the OPD was also measured. Fig. 4(a) shows the time-dependent photocurrent caused by resorufin through the enzymatic reaction with the free HRP–APnEOs and the HRP–APnEOs that were immobilized on the magnetic microbeads (0.4 mg) in Tris–HCl buffer (2.0 mL, pH=8.0). The initial velocity (ν) was calculated from the initial slope in Fig. 4(a) and the initial velocity was plotted against the concentration of the HRP–APnEOs conjugate ($c_{HRP-APnEOs}$), as shown in Fig. 4(b). A good linear relationship was observed between the initial velocity and the concentration of HRP–APnEOs in the range from 1.0 to 2.5 ppb. It seems that at 0.25 ppb of HRP–APnEOs conjugate, no enzymatic reaction occurred. This may be explained by inactivation of HRP at higher concentration of H_2O_2 [31b]. The initial velocity for the HRP–APnEOs conjugate immobilized on the magnetic microbeads incubated in 500 ppb HRP–APnEOs solution was 2.5 nM s^{-1}, and which corresponds to that for a 1.0 ppb concentration of the HRP–APnEOs conjugate solution. Judging from the initial velocity for the HRP–APnEOs conjugate solution (that is, from the fact that the initial velocity of 2 mL of 1 ppb HRP–APnEOs and HRP–APnEOs on 0.4 mg magnetic microbeads are almost same), we obtained apparent amount of HRP–APnEOs antibody on the magnetic microbeads as 5.0 ng mg^{-1} assuming the activity of free and HRP–APnEOs conjugate on the magnetic microbeads is same. To measure a lower photocurrent by the ELISA, the yellow LED was inadequate because of the relatively higher background photocurrent, even when a band pass filter was used. Therefore we used an LED with λ=505 nm as a light source for the competitive ELISA.

Fig. 5(a) shows time-dependent photocurrent data, obtained for the competitive ELISA for the APnEOs. After adding the mixture of APnEOs (0–100 ppb) and HRP–APnEOs (500 ppb) conjugate to the magnetic microbeads immobilized with the anti-APnEOs antibody followed by incubation, the Amplex Red solution containing H_2O_2 was added to the suspension of the magnetic microbeads. The photocurrent then increased lineally against time, as shown in Fig. 5(a). The increase in photocurrent with time is due to the generation of fluorescent resorufin from the Amplex Red as the result of the enzymatic reaction with HRP labeled APnEOs and H_2O_2. A plot of the photocurrent values at t=500 s against the concentration of APnEOs in the incubation solution is shown in Fig. 5(b). In this case, the photocurrent values were normalized by the photocurrent value obtained for the incubation solution without APnEOs (c_{APnEOs}=0 ppb). The photocurrent decreased dramatically in the concentration range of 5–50 ppb for the APnEOs.

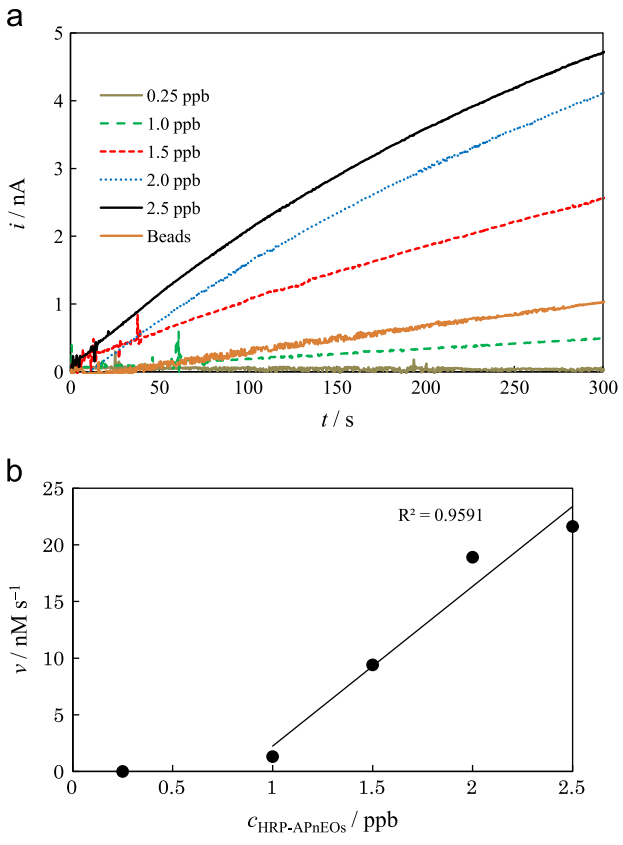

Fig. 4. (a) Time-dependent photocurrent of OPD by fluorescent resorufin through the enzymatic reaction of Amplex Red with H_2O_2 and HRP–APnEOs (0.25, 1.0, 1.5, 2.0, and 2.5 ppb, and 0.4 mg magnetic microbeads with anti-APnEOs antibody incubated in a 500 ppb HRP–APnEOs solution), and (b) the initial velocity of the enzymatic reaction as a function of the concentration of HRP–APnEOs. An LED light with λ=591 nm was employed.

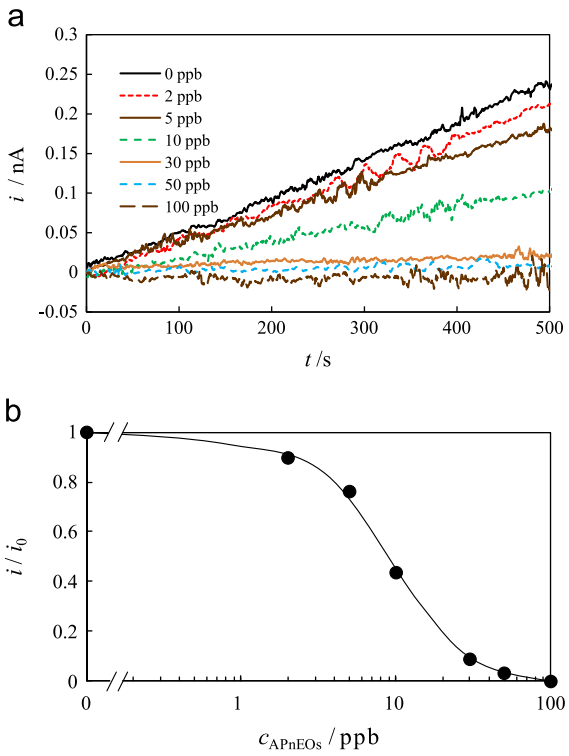

Fig. 5. (a) Time-dependent photocurrent of the OPD during a competitive ELISA of APnEOs (0, 2, 5, 10, 30, 50, and 100 ppb) and the HRP-APnEOs conjugate (500 ppb). (b) Photocurrent values at 500 s after addition of a mixture of Amplex Red and H_2O_2. The photocurrent is normalized by that at c_{APnEOs}=0 ppb. The solid line is to guide the eye. An LED with λ=505 nm was employed as a light source.

It is possible to accurately determine the concentration of APnEOs in this concentration range. From Fig. 5(b), the binding constants of the anti-APnEOs antibody immobilized on the magnetic microbeads with APnEOs (K_1) or the HRP–APnEOs conjugate (K_2) in the incubation solution can be estimated by simulation of an adsorption model [32] (Supplementary). The apparent values of K_1 and K_2 were in the range of 2.0×10^8–1.5×10^9 M^{-1} and 1.0×10^7–1.0×10^8 M^{-1}, respectively (Fig. S3). These results appear to be reasonable, judging from the molecular weights of the APnEOs and HRP–APnEOs conjugate. Namely, in case of the HRP–APnEOs conjugate having a larger molecular weight, steric hindrance may play a role in the immunoreactions with the antibody on the magnetic microbeads and could affect the overall reaction rates. We estimated values for surface coverage of the anti-APnEOs antibody on the magnetic microbeads by HRP–APnEOs for the better understanding of immunoreaction. The surface coverage of anti-APnEOs antibody by HRP–APnEOs conjugate is a function of K_1, K_2, and c_{APnEOs} when $c_{HRP-APnEOs}$ is constant (Fig. S4). Using reasonable values of K_1 and K_2, the values of surface coverage were estimated to be 5.6 (at $K_1=1.5\times10^9$ $M^{-1}$and $K_2=1.0\times10^7$ M^{-1}) and 86% (at $K_1=1.0\times10^7$and $K_2=1.0\times10^8$ M^{-1}).

3.3. Flow injection fluorometric immunoassay for APnEOs by using the magnetic microbeads immobilized with antibody

The results using a batch system suggest that this OPD system can be used in a flow system for a fluorometric immunoassay, a process that requires sequential operations. The results of the batch system provide us with guidelines for the construction of the flow system. We used 0.2 mg of microbeads and a magnet ($d=3.0$ mm), which was placed under the microchip. Once the magnetic microbeads are trapped by the magnet in the microchannel, it is possible to carry out the successive procedures that make up a competitive ELISA such as the introduction of the sample solution and the Amplex Red solution. At the injection process of magnetic microbeads, the magnetic microbeads hardly blocked the channel because of smaller diameter compared with the channel width and depth.

The time-dependent response of the photocurrent of the OPD was obtained when 100 μL of the Amplex Red solution containing H_2O_2 was injected into the carrier stream at a flow rate of 20 μL min^{-1}. The results are shown in Fig. 6. The photocurrent gradually increased at around $t=100$ s after the injection of the Amplex Red solution and reached a maximum at around $t=250$–350 s and then gradually decreased, finally returning to the baseline (Fig. 6(a)). Since the volume of the Amplex Red solution and the flow rate of the carrier solution are 100 μL and 20 μL min^{-1}, respectively. Approximately 300 s is needed for the injected sample to pass through the microchannel. Therefore, the photocurrent–time range in Fig. 6(a) is reasonable. The photocurrent observed at $t=250$–350 s may reflect the steady state for the enzymatic reaction of HRP on the magnetic microbeads with Amplex Red and H_2O_2. Therefore, the photocurrents for 30 s observed at around $t=300$ s were averaged and the average values were plotted against the concentration of APnEOs. In this case, the photocurrent was normalized by that obtained for the sample solution at $c_{APnEOs}=0$ ppb (Fig. 6(b)). It can be seen that the photocurrent decreased dramatically for the APnEOs in the concentration range between 4 and 15 ppb. The determinable concentration range for the flow system is comparable to that for the batch system (2–20 ppb) and the estimated values for the binding constants, K_1 and K_2 were identical (Fig. S3). The sample throughput was 4–5 samples for 1 h in the flow system.

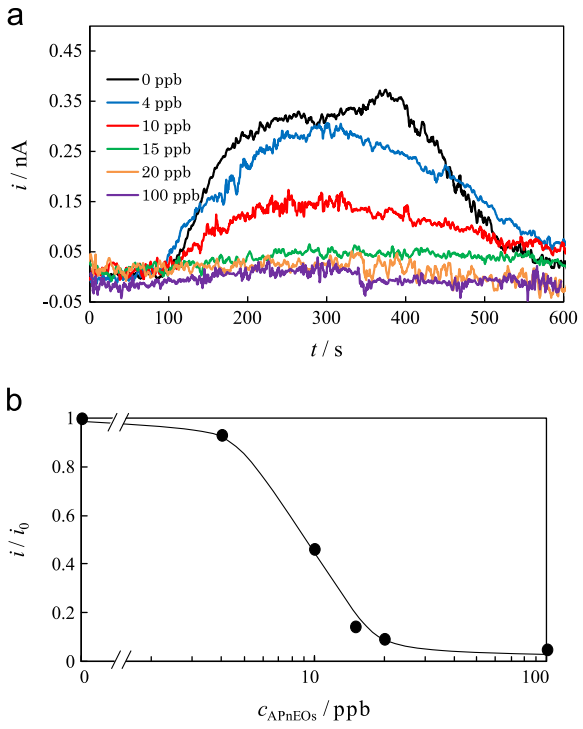

Fig. 6. (a) Time-dependent photocurrent of OPD by competitive flow ELISA of APnEOs (500 ppb) and HRP–APnEOs conjugate (0, 4, 10, 15, 20, and100 ppb). (b) Photocurrent values at $t=300$ s after injection of a mixture of Amplex Red and H_2O_2. The photocurrent is normalized by that at $c_{APnEOs}=0$ ppb. The solid line is to guide the eye. An LED with $\lambda=505$ nm was employed as a light source. A typical standard deviation was 7%.

4. Conclusions

We report on the assembling of an optical system combined an LED with a fabricated OPD for the fluoromeric detection of an analyte on a microchip and successfully conducted a flow fluorometric immunoassay for APnEOs. Recently, research dealing with OPDs have increased and have become popular, since the OPDs are suitable for use as a spectroscopic detection device for μ-TAS. OPDs are compact and can be tuned by appropriate adjustment of the organic layers used in their construction. Therefore OPDs as well as inorganic photodiodes represent promising devices for use as a portable photodetection for μ-TAS. The fabricated OPD has the capacity to efficiently convert the fluorescence of resorufin into a photocurrent. The detection limits of the APnEOs were 2 and 4 ppb for batch and flow systems, respectively. These values are comparable with previous work for the detection of APnEOs by capillaries [33], chromatographic [34], chemiluminescence [35], SPR iimunoassay [36] whose detection limit is in the range of a few ppb to 10 ppb. In our study, such low detection limits can be attributable to, not only the performance of the OPD, but also the higher affinity between the anti-APnEOs antibody immobilized on the magnetic microbeads and antigens. The apparent affinities of the anti-APnEOs antibody immobilized on the magnetic microbeads, APnEOs ($K_1=2.0\times10^8$–1.5×10^9 M^{-1}) and HRP–APnEOs ($K_2=1.0\times10^7$–1.0×10^8 M^{-1}), were found to be sufficiently high to permit low concentrations of APnEOs to be detected.

Acknowledgments

This work was supported in part by the Funding Program for World-Leading Innovative R&D on Science and Technology (FIRST).

Appendix A. Supplementary material

Supplementary data associated with this article can be found in the online version at http://dx.doi.org/10.1016/j.talanta.2013.08.044.

References

[1] H. Becker, L.E. Locascio, Talanta 56 (2002) 267.
[2] T. Kamei, B.M. Paegel, J.R. Scherer, A.M. Skelley, R.A. Street, R.A. Mathies, Anal. Chem. 75 (2003) 5300.
[3] T. Kamei, T. Wada, Appl. Phys. Lett. 89 (2006) 114101.
[4] F. Yang, X.C. Li, W. Zhang, J.B. Pan, Z.G. Chen, Talanta 84 (2011) 1099.
[5] J. Wu, X. Liu, L. Wang, L. Dong, Q. Pu, Analyst 137 (2012) 519.
[6] D. Kearns, M. Calvin, J. Chem. Phys. 29 (1958) 950.
[7] C.W. Tang, Appl. Phys. Lett. 48 (1986) 183.
[8] P. Peumans, A. Yakimov, S.R. Forrest, J. Appl. Phys. 93 (2003) 3693.
[9] H. Spanggaard, F.C. Krebs, Sol. Energy Mater. Sol. C 83 (2004) 125.
[10] B.P. Rand, J. Genoe, P. Heremans, J. Poortmans: Sol. Cells 15 (2007) 659.
[11] E. Engvall, P. Perlmann, Immunochemistry 8 (1971) 871.
[12] X. Wang, M. Amatatongchai, D. Nacapricha, O. Hofmann, J.C. de Mello, D.D. C. Bradley, A.J. de Mello, Sensors Actuat. B: Chem. 140 (2009) 643.
[13] A. Banerjee, Y. Shuai, R. Dixit, I. Papautsky, D. Klotzkin, J. Lumin. 130 (2010) 1095.
[14] O. Hofmann, P. Miller, P. Sullivan, T.S. Jones, J.C. deMello, D.D.C. Bradley, J. Andrew, Sensors Actuat. B: Chem. 106 (2005) 878.
[15] A. Banerjee, A. Pais, I. Papautsky, D. Klotzkin, IEEE Sensors J. 8 (2008) 621.
[16] J.R. Wojciechowski, L.C. Shriver-Lake, M.Y. Yamaguchi, E. Füreder, R. Pieler, M. Schamesberger, C. Winder, H.J. Prall, M. Sonnleitner, F.S. Ligler, Anal. Chem. 81 (2009) 3455.
[17] M. Miyake, H. Nakajima, A. Hemmi, M. Yahiro, C. Adachi, N. Soh, R. Ishimatsu, K. Nakano, K. Uchiyama, T. Imato, Talanta 96 (2012) 132.
[18] H.R.M. Far, F. Torabi, B. Danielsson, M. Khayyami, J. Anal. Toxicol. 29 (2005) 790.
[19] H. Miyaguchi, H. Takahashi, T. Ohashi, K. Mawatari, Y.T. Iwata, H. Inoue, T. Kitamori, Forensic Sci. Int. 184 (2009) 1.
[20] S.J. Hu, M.T. French, D.A. Palmer, M. Evans, S.M. Zhou, G.H. Sarpara, J.N. Miller, Anal. Chim. Acta 454 (2002) 31.
[21] S. Kim, J.K. Park, Biotechnol. Bioprocess Eng. 9 (2004) 127.
[22] A.T. Pereira, P. Novo, D.M.F. Parazeres, V. Chu, J.P. Conde, Biomicrofluidics 5 (2011) 014102.
[23] (a) R. Renner, Environ. Sci. Technol. 31 (1997) 316A;
(b) Chemical substance fact sheets, Ministry of Environment, Government of Japan, 2012. Available from: ⟨http://www.env.go.jp/chemi/communication/factsheet.html⟩;
(c) Alkylphenol ethoxylate, The Soap and Detergent Association, 1999;
(d) Chemical risk information platform, Incorporated Administrative Agency National Institute of Technology and Evaluation. Available from: ⟨http://www.safe.nite.go.jp/english/sougou/view/IntrmSrchYusenList_en.faces⟩.
[24] Y. Goda, A. Kobayashi, S. Fujimoto, Y. Toyoda, K. Miyagawa, M. Ike, M. Fujita, Water Res. 38 (2004) 4323.
[25] M. Hiramoto, H. Fujiwara, M. Yokoyama, Appl. Phys. Lett. 58 (1991) 1062.
[26] M. Hiramoto, H. Fukusumi, M. Yokoyama, Appl. Phys. Lett. 61 (1992) 2580.
[27] P. Peumans, S.R. Forrest, Appl. Phys. Lett. 79 (2001) 126.
[28] Y. Kinoshita, T. Hasobe, H. Murata, Appl. Phys. Lett. 91 (2007) 083518.
[29] S. Solè, A. Merkoçi, S. Alegret, Trends Anal. Chem. 20 (2001) 102.
[30] K. Hirakawa, M. Katayama, N. Soh, K. Nakano, T. Imato, Anal. Sci. 22 (2006) 81.
[31] (a) M. Zhou, Z. Diwu, N. Panchuk-Voloshina, R.P. Haugland, Anal. Biochem. 253 (1997) 162;
(b) M.B. Arnao, M. Acosta, J.A.D. elRío, R. Varón, F. García-Cánovas, Biochim. Biophys. Acta 1041 (1990) 43.
[32] R. Zhang, H. Nakajima, N. Soh, K. Nakano, T. Masadome, K. Nagata, K. Sakamoto, T. Imato, Anal. Chim. Acta 600 (2007) 105.
[33] A. Rose, C. Nistor, J. Emnéus, D. Pfeiffer, U. wollenberger, Biosensors Bioelectron. 17 (2002) 1033.
[34] M. Badea, C. Nistor, Y. Goda, S. Fujimoto, S. Dosho, A. Danet, D. Barceló, F. Ventura, J. Emnéus, Analyst 128 (2003) 849.
[35] R. Zhang, H. Nakajima, S. Nobuaki, K. Nakano, T. Masadome, K. Nagata, K. Sakamoto, T. Imato, Anal. Chim. Acta 600 (2007) 105.
[36] M. Tanaka, K. Sakamoto, H. Nakajima, N. Soh, K. Nakano, T. Masadome, T. Imato, Anal. Sci. 25 (2009) 999.